Self-coupled optical waveguide (SCOW) resonators for optical signal processing

Linjie Zhou*, Shulin Li, Jingya Xie, Qianqian Wu, and Jianping Chen
State Key Laboratory of Advanced Optical Communication Systems and Networks
Department of Electronic Engineering, Shanghai Jiao Tong University, Shanghai 200240, China

*Email: ljzhou@sjtu.edu.cn

ABSTRACT

We investigate the optical signal processing capability of self-coupled optical waveguide (SCOW) resonators. Benefited from the double-notch resonance feature in transmission, a variety of optical pulse shaping functions can be implemented. A Gaussian input pulse can be transformed to a flat-top square-like pulse or in reverse. The separate and merged notches can perform first- and second-order differentiations to the input pulse. Odd-symmetry Hermite-Gaussian (OS-HG) waveforms are generated from the differentiation. Numerical simulation and preliminary experimental results are given.

Keywords: silicon photonics, resonators, waveguides, optical signal processing, optical filters, optical pulse shaping

1. INTRODUCTION

All-optical signal processing has attracted great research interest in recent years, as it can overcome the bandwidth and power limitation imposed by electronic processing systems. One of the important functions in optical signal processing is the pulse shaping, a conversion of input pulses to well-defined temporal waveforms and sequences. It can be performed either in the frequency domain or directly in the temporal domain. As for the former, linear filtering devices are most commonly used. They control the amplitude and phase of the frequency components of a short pulse to enable the pulse waveform tailoring in the time domain. Direct temporal reshaping based on nonlinear pulse propagation or real-time signal transform is also a viable solution. Multiple mechanisms and devices can be employed for optical pulse shaping, including SiN microring frequency combs for line-by-line processing [1], silicon waveguides and gratings for nonlinear spectral broadening and dispersion [2], fiber gratings or directional couplers for temporal differentiation [3, 4], fiber Bragg gratings for temporal Hilbert transform (THT) [5], single or cascaded microring resonators for signal conversion or differentiation [6-8], and microring resonators for temporal integration [9].

Previously, we proposed and demonstrated a novel self-coupled optical waveguide (SCOW) resonator formed by a waveguide with two folding points [10-14]. The SCOW resonators are standing-wave resonators with both the clockwise (CW) and the counterclockwise (CCW) modes being co-excited. This makes them distinct from regular microring resonators. The CW and CCW modes are sequentially excited without direct coupling. Split and enhanced resonance notches are observed from the SCOW resonator transmission spectrum [10, 11]. When two SCOW resonators are cascaded in series, coupled-resonator-induced transparency (CRIT) effect can be generated [12]. In this paper, we explore its pulse shaping capability based on its unique resonance features. We first present the numerical simulations using the transfer equation of the SCOW resonator. It is demonstrated that the SCOW resonator can convert a Gaussian pulse to a flat-top pulse or the reverse by properly setting the coupling coefficients. Using the differentiation property of the single or double notches, a single Gaussian pulse can also be converted to consecutive double pulses with either in-phase or anti-phase. We then present our preliminary experimental results using a passive silicon SCOW resonator. The experimental results agree well with the theoretical predictions.

Silicon Photonics IX, edited by Joel Kubby, Graham T. Reed, Proc. of SPIE Vol. 8990, 89901F
 · doi: 10.1117/12.2039906

2. MODELING AND SIMULATIONS

Figure 1 shows the schematic structure of the SCOW resonator with two couplers of identical or different coefficients. The coupling coefficients are denoted as κ_1 and κ_2, and the corresponding transmission coefficients are t_1 and t_2, respectively. Assuming the coupling is lossless, we have $t_i^2+\kappa_i^2=1$ (i = 1, 2). Because of the twist structure of the SCOW resonator, the clockwise (CW) and counter-clockwise (CCW) resonance modes are both excited. Benefited from its unique resonance feature, various pulse shaping processes can be done using the SCOW resonator. Figure 1(b) depicts the input Gaussian pulse that we will use in our calculation. The pulse is unchirped with a constant phase. The peak power is 1 mW (to exclude any nonlinear process) and the full pulse width (defined as the 1/e power point) is 10 ps. The input pulse energy is 88.62 fJ. The transfer function of the SCOW resonator can be deduced from the transfer matrix method [10]:

$$H(\omega) = -e^{-i\beta L_b}\left[\frac{(\kappa_1 - \kappa_2 a e^{-i\beta L})(\kappa_2 - \kappa_1 a e^{-i\beta L})}{(1-\kappa_1\kappa_2 a e^{-i\beta L})^2} + \left(\frac{t_1 t_2 a^{1/2} e^{-i\beta L/2}}{1-\kappa_1\kappa_2 a e^{-i\beta L}}\right)^2\right] \quad (1)$$

where $L = L_1+L_2$ is the round-trip length of the SCOW resonator, L_b is the length of the central bridge waveguide, a is the loss factor, and $\beta = n_{eff}\omega/c$ is the propagation constant of the waveguide. Resonance occurs when $\beta L = 2m\pi$ (m is an integer number). Figure 1(c) shows the typical transmission spectrum of a symmetric SCOW resonator with the coupling coefficients both being κ = 0.97. The resonator size is L = 50 μm and the loss factor is a = 0.999 (corresponding to 1.7 dB/cm waveguide propagation loss). The effective index of a typical 500 nm × 220 nm silicon waveguide is n_{eff} = 2.52. The transmission spectrum exhibits a transparency peak at the resonance wavelength (λ_0= 1546 nm). Beside the peak is the two deep notches.

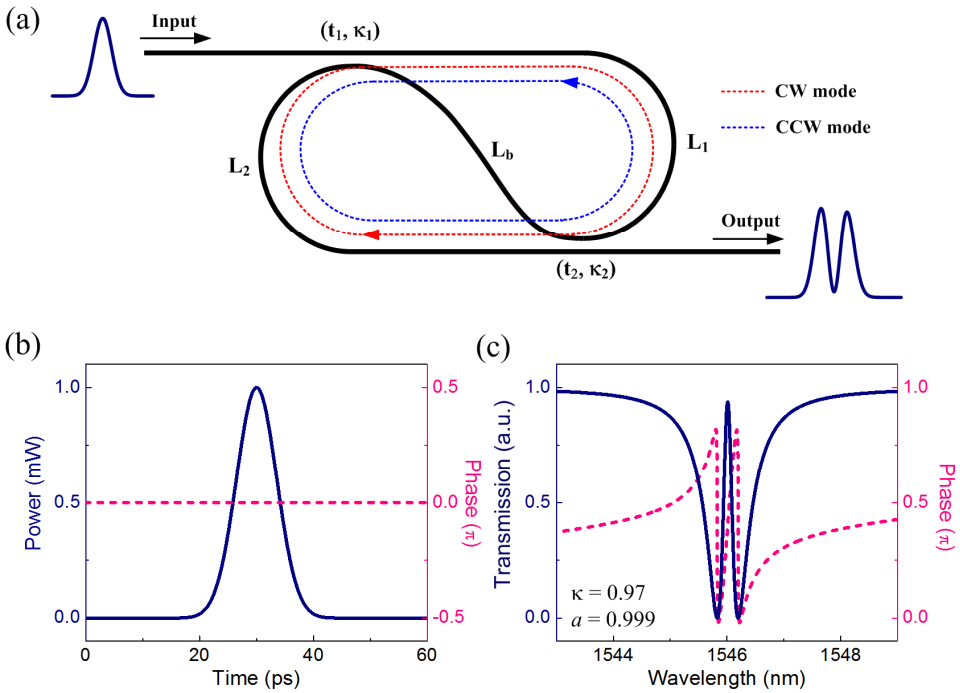

Figure 1. (a) Schematic of the SCOW resonator. (b) Temporal waveform of the input Gaussian pulse. (c) Typical power and phase transmission spectra of a symmetric SCOW resonator.

The W-shaped SCOW resonance spectrum can be used to tailor the input pulse. We first set the pulse carrier wavelength exactly at the resonance wavelength. Depending on the coupling coefficient, the separation of the two notches can be varied. Hence, it can attenuate different frequency components of the input pulse spectrum. Figure 2 shows the pulse shaping results using three symmetric SCOW resonators with different coupling coefficients. If the coupling is weak (κ= 0.9), the deep notches are close to the edge of the input pulse spectrum. As a result, the pulse spectrum becomes narrower and its temporal waveform becomes broader with a width of 13.4 ps. When the coupling increases (κ= 0.95), the notches

are closer to the carrier wavelength, generating two small sidelobes. As we known, Fourier transform of a square pulse results in a sinc function. The tailored pulse spectrum (Fig. 2(e)) resembles a sinc function, thereby generating a more square-like pulse in the temporal domain. If the coupling is even stronger (κ= 0.97), the sidelobes grow up to take a significant power. In this case, the output pulse is split into two in phase. It should be noted that the pulse power reduces with the increasing coupling coefficient as more central components are filtered out.

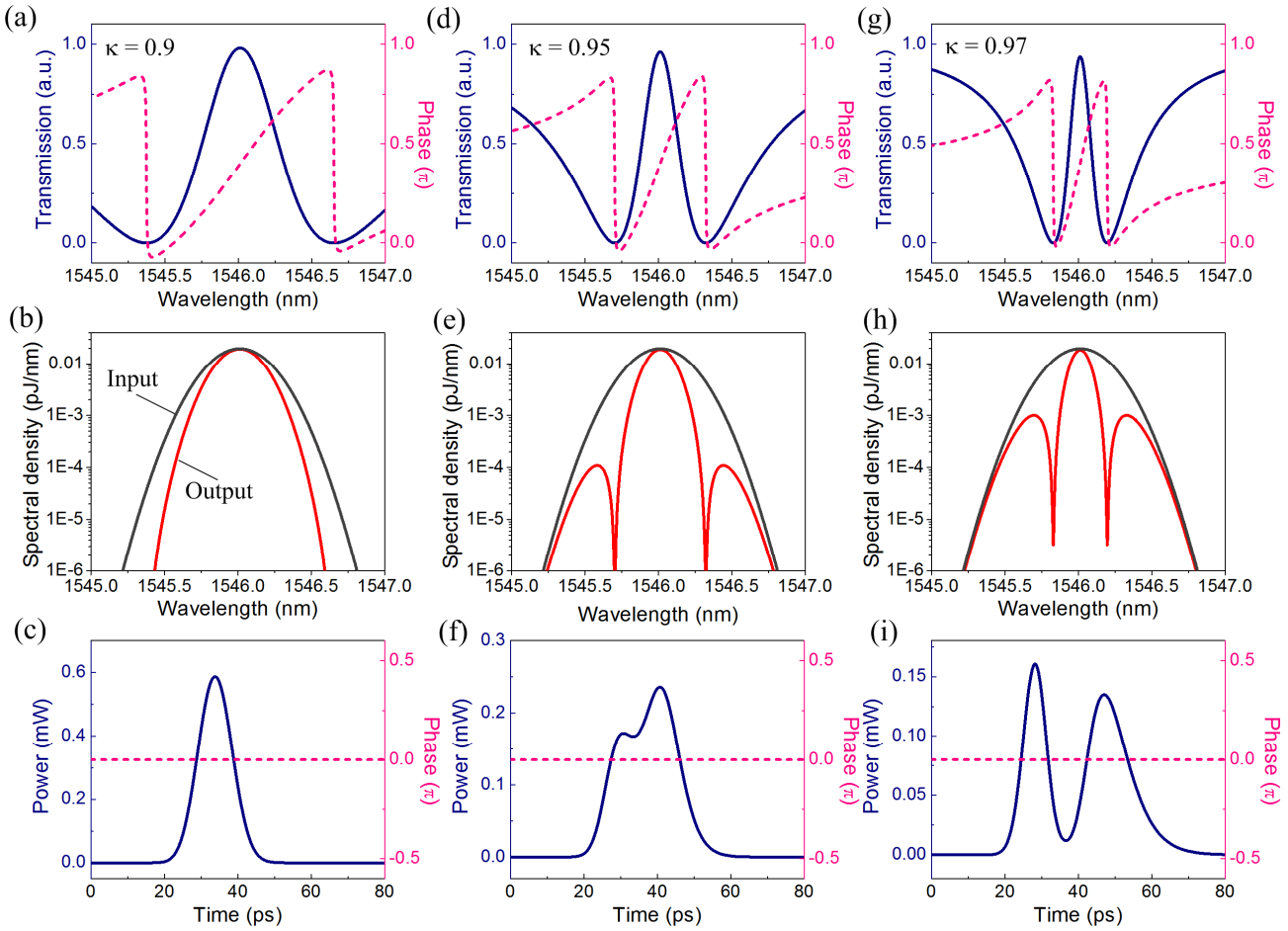

Figure 2. Pulse shaping using symmetric SCOW resonators. The carrier wavelength of the input Gaussian pulse is at the resonance wavelength. The top plots are the SCOW resonator transmission spectra, the middle ones are the input and output pulse spectra, and the bottom ones are the resultant output pulse temporal waveforms. Coupling coefficients are set as (a)-(c) κ= 0.9, (d)-(f) κ= 0.95, and (g)-(i) κ= 0.97.

Although the input pulse can be tailored into various shapes by tuning the coupling coefficients of a symmetric SCOW resonator, it is hard to get a flat-top square-like pulse. In order to further fatten the pulse, the relative weight of the central peak and sidelobes need to be adjusted. In this regard, we need to use asymmetric SCOW resonators of which the central transparency peak can be varied as shown in Fig. 3. Since there are two degrees of freedom, the pulse spectrum can be more easily tailored to approach a sinc function. The resultant pulse has a fairy flat top and the pulse also widened to 18 ps. The flat-top optical pulses are highly desirable for a variety of applications, including optical gating, nonlinear optical switching, and frequency conversion applications etc. [15, 16].

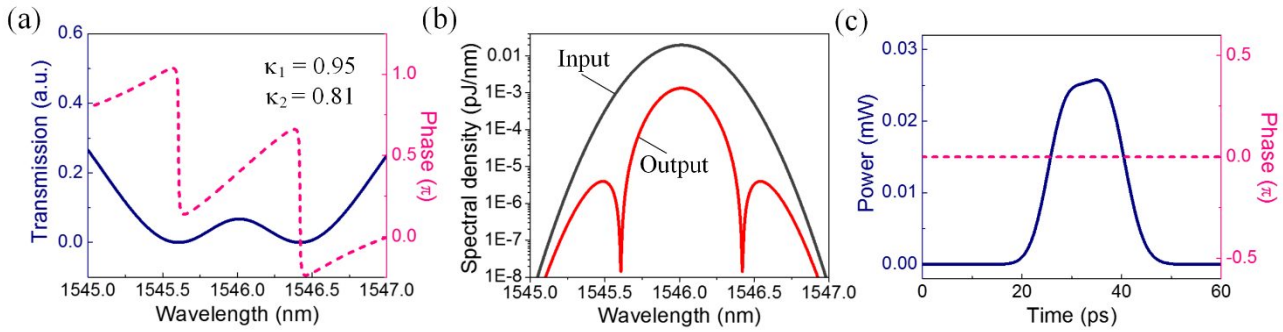

Figure 3. Pulse shaping using an asymmetric SCOW resonator. (a) SCOW resonator transmission spectrum. (b) Input and output pulse spectra. (c) Output pulse temporal waveform. The pulse carrier wavelength is at the SCOW resonance wavelength.

A square pulse can also be converted into a Gaussian-like pulse using the SCOW resonator. For such a conversion, the two notches in the SCOW spectrum need to be placed at the first sidelodes of the square pulse spectrum as shown in Fig. 4. The square pulse spectrum is truncated by the two deep notches of the SCOW resonator with more than 10 dB attenuation for the first sidelobes. Since the central main peak is remained, the pulse energy is not significantly lost with the energy efficiency (energy ratio between output and input pulses) being 0.8. A microring resonator can also perform a similar function, but it has limited attenuation because the Lorenzian resonance lineshape has more gentle transition edges.

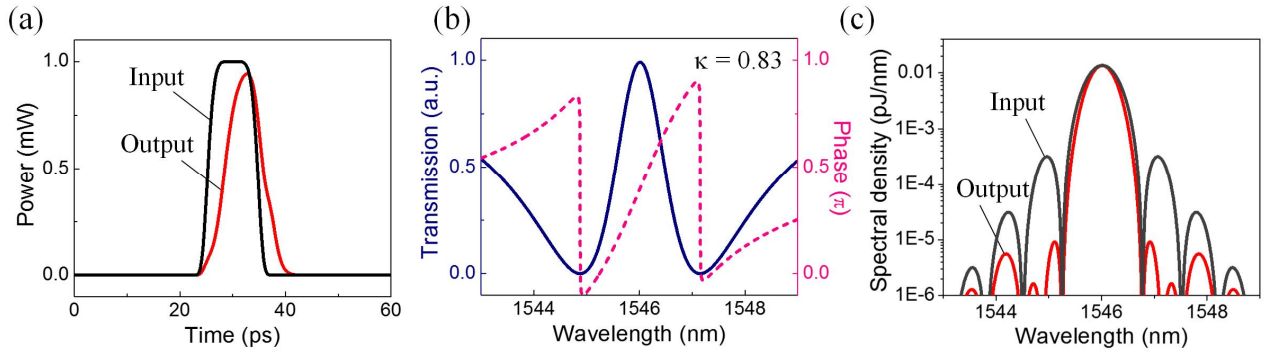

Figure 4. Pulse sharping using a symmetric SCOW resonator. The input is a square pulse with its carrier wavelength at the resonance wavelength. (a) Temporal waveforms of the input and output pulses. (b) Transmission spectrum of the SCOW resonator. (c) Input and output pulse spectra.

We next explore the pulse shaping when the carrier wavelength is detuned to the notch wavelength as shown in Fig. 5. The configurations of the SCOW resonators are the same with those used in Fig. 2. For low coupling (κ= 0.9) and large separation of the notches, only the carrier frequency is removed. The remained two sidelobes compose the resultant double pulses. The pulse separation is ~10.3 ps. There is a π-phase shift between these two consecutive pulses. As for the individual notch, the SCOW resonator can be regarded as a first-order filter. The transfer function can be approximated as a linear function of the frequency detuning from the notch. Therefore, the SCOW resonator works as a first-order differentiator. The typical waveform is an odd-symmetry Hermite-Gaussian (OS-HG) waveform, consisting of two linked π-phase-shifted temporal pulses [17]. This waveform is called a 'soliton molecule', an approximation of the second-order dispersion-managed temporal soliton [18]. It can be used as a new communication symbol to increase the information carrier capacity of the fiber optics systems. With the increase in coupling, the other notch also acts on the pulse spectrum. In particular, the pulse spectrum is divided into three lobes when κ= 0.97, breaking the symmetry of the output waveform. The tailing pulse is weaker and broader than the leading pulse. The increased coupling reduces the resonance bandwidth, so that the transfer function cannot be well defined by a linear function in the pulse bandwidth, leading to more deviation from the ideal OS-HG waveform.

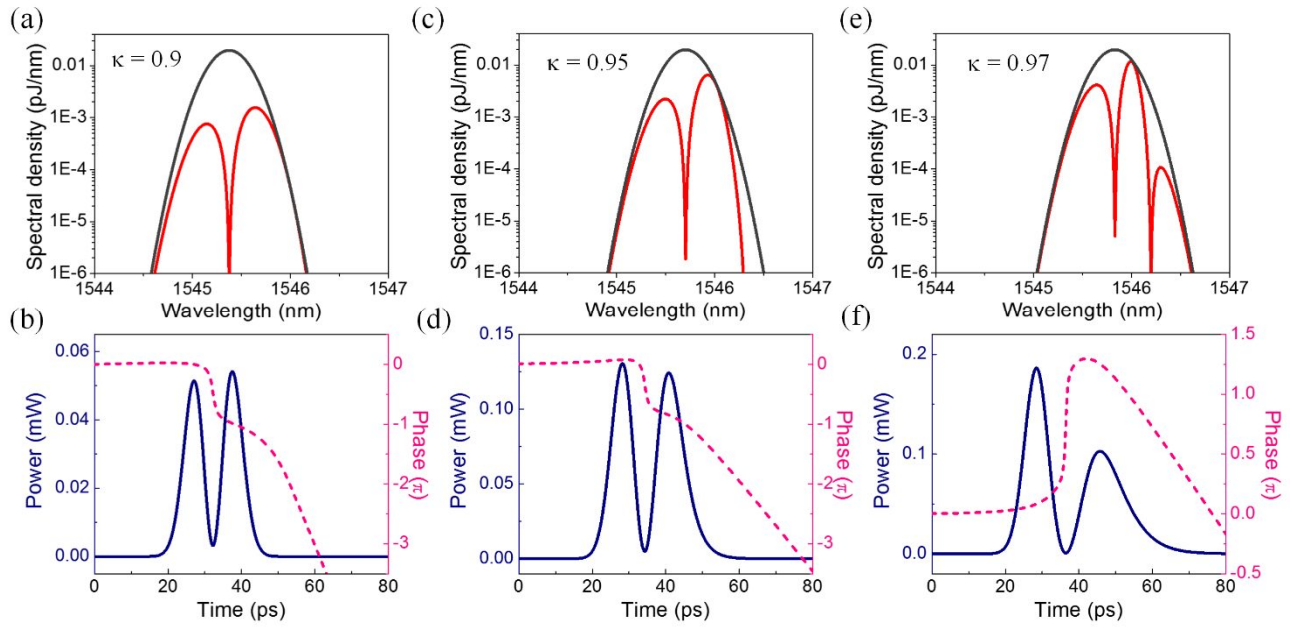

Figure 5 First-order differentiation using separated notches of a symmetric SCOW resonator. The pulse carrier wavelength is set at the left notch wavelength. The top plots show the spectra of the input and output pulses. The bottom plots are the corresponding output temporal waveforms.

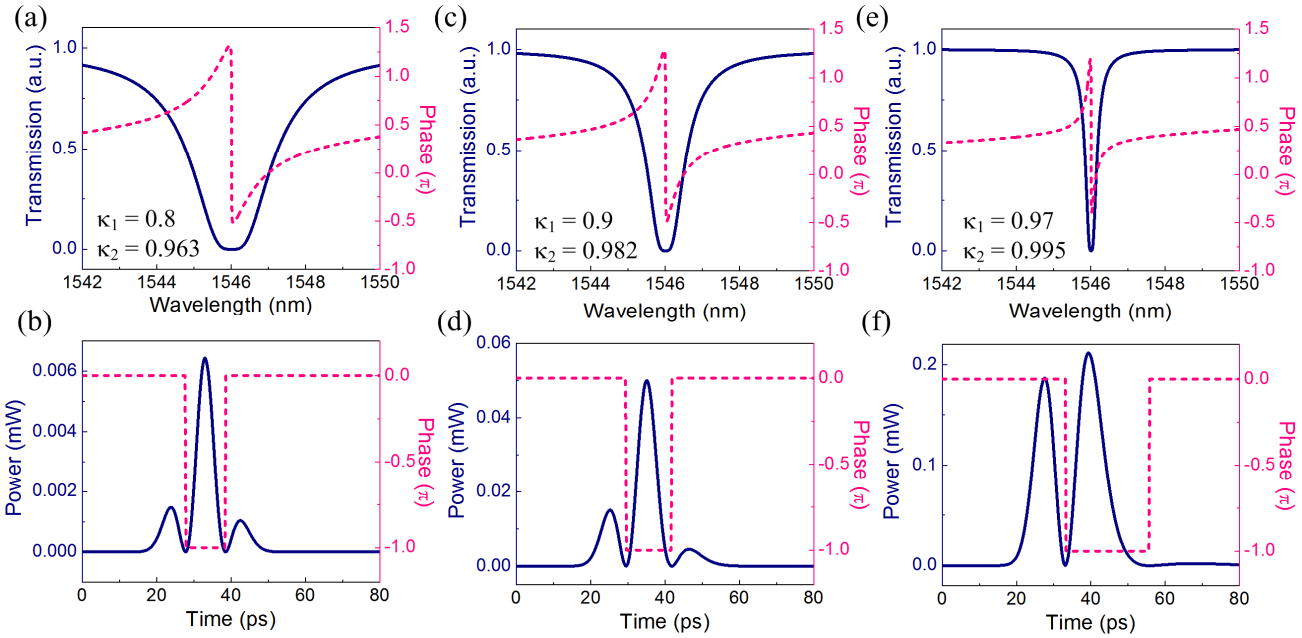

Figure. 6 Second-order differentiation using the merged notch of an asymmetric SCOW resonator. The pulse carrier wavelength is set at the resonance wavelength. The top plots show the transmission spectra of three SCOW resonators. The bottom plots are the corresponding output temporal waveforms.

For the symmetric SCOW resonators, the separate notches can work as two independent first-order differentiators. On the other hand, we can think of merging these two notches so that the two differentiators operate at the same wavelength. In this sense, it becomes a second-order differentiator. In order to merge these two notches, we need to use asymmetric SCOW resonators and their coupling coefficients should satisfy $|\kappa_1 - \kappa_2| = t_1 t_2$ [10]. Figure 6 shows the pulse shaping results using three asymmetric SCOW resonators with various notch bandwidths. Similar to the first-order differentiation, the

SCOW transfer function can be well approximated by a quadratic function of frequency detuning if the resonance bandwidth is larger than the pulse bandwidth ($\kappa_1 = 0.8$, $\kappa_2 = 0.963$). In this case, the resultant waveform is closer to the ideal second-order differentiation waveform composed of one main peak and two π-phase shifted small side peaks. With the narrower notch, more energy is carried from the tailing peak to the leading peak. Specifically, when $\kappa_1 = 0.97$ and $\kappa_2 = 0.995$, the tailing peak almost disappears while the leading one grows to a comparable power level with the central one. Such a waveform is similar to the OS-HG waveform as in the first-order differentiator.

3. EXPERIMENTS

We fabricated a passive symmetric SCOW resonator on a silicon-on-insulator (SOI) substrate using silicon microelectronics fabrication processes. The silicon waveguide width is 450 nm and the height is 220 nm. The etched depth of the waveguide is 160 nm with a 60 nm slab. Gratings are used at the end of the waveguide for input and output coupling. To ensure a large coupling coefficient, directional couplers are employed for the two couplers of SCOW resonator. The coupling length is 20 μm with a gap size of 0.2 μm. We measured the transmission spectrum using the Agilent loss and dispersion analyzer (86038B). The input light was transverse-electrically (TE) polarized by using a polarizer controller before the device.

Figure 7 shows the transmission spectrum of the SCOW resonator. The resonance free-spectral range (FSR) is around 2.8 nm. Two deep notches with an extinction ratio of 20 dB are clearly observed for each resonance. The notch separation is 0.13 nm for the 1542.58 nm resonance. The 3-dB bandwidth of each notch is around 0.12 nm.

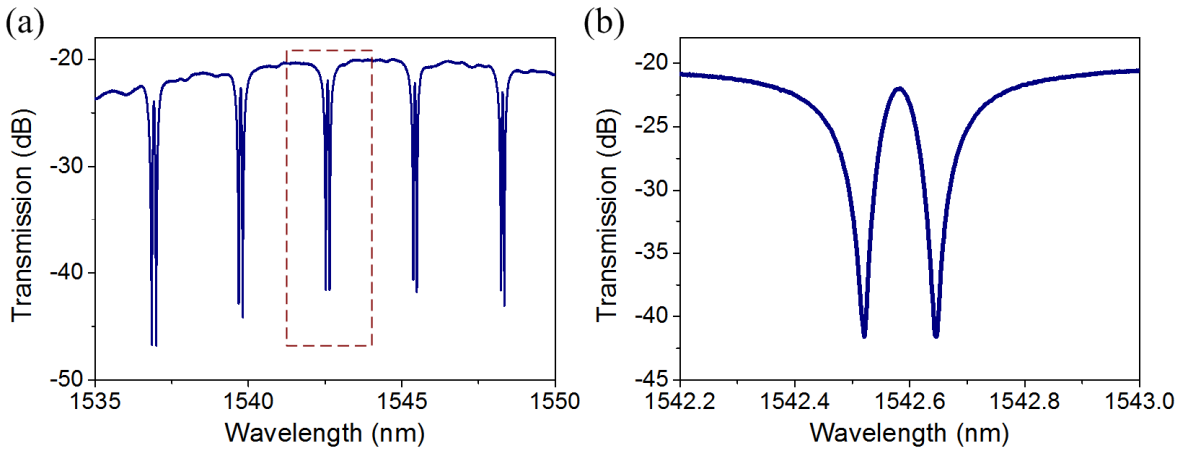

Figure. 7 (a) Measured transmission spectrum of a symmetric SCOW resonator. (b) Zoom-in view of one resonance around 1542.58 nm.

Figure 8 shows our preliminary pulse shaping results. In one experiment, we used a Gaussian input pulse with a width of 90 ps and the carrier wavelength is tuned to the left notch at 1542.52 nm. As discussed in the previous section, the SCOW resonator works as a first-order differentiator in this case. The double-pulse waveform is output from the device as shown in Fig. 8(a), consistent with the theoretical prediction. The constituent pulse width is 45 ps and the relative delay is 70 ps. In another experiment, we transmitted a 0.38 ns wide square pulse through the device and the result is shown in Fig. 8(b). With the sidelobes suppressed by the notches, the square pulse is transformed into a Gaussian-like pulse. The pulse width is 0.43 ns.

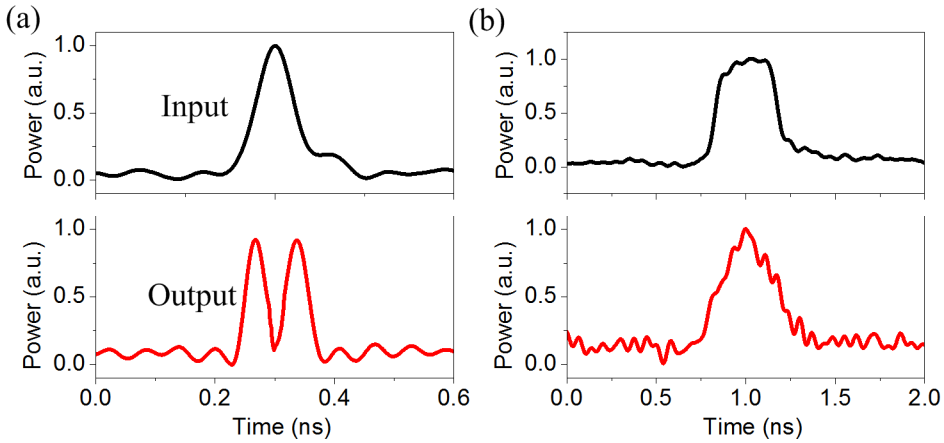

Figure. 8 Experimental results for pulse shaping. (a) Input Gaussian pulse is differentiated into an OS-HG pulse. (b) Input square pulse is transformed into a Gaussian-like pulse.

4. CONCLUSIONS

The SCOW resonator differs from a single microring resonator in terms of resonance modes and transmission spectrum. Because of the co-excitation of the CW and CCW modes in the resonator, their interference at the output port results in the typical double-notch resonance spectrum. It should be noted that the double-notch resonance mechanism is different from the resonance splitting in coupled resonators [19, 20]. A particular useful feature of the SCOW resonator is that the notch separation and the central transparency peak can be freely set by tuning the two coupling coefficients, which can be used to transform the input pulse to various forms. Our study shows that a Gaussian input pulse can be reshaped into a flat-top square-like pulse or two consecutive pulses in phase. A square pulses can also be converted to a Gaussian-like pulse upon truncating the spectral sidelobes. The frequency components of the input pulse are manipulated to enable the transformation. Around the transmission notch, the SCOW resonator can work as a first- or second-order temporal differentiator, which is particularly useful for optical computing. An odd-symmetry Hermite-Gaussian (OS-HG) waveform can be derived from the original Gaussian pulse.

5. ACKNOWLEDGEMENTS

This work was supported in part by the 973 program (ID2011CB301700), the 863 program (2013AA014402), the National Natural Science Foundation of China (NSFC) (61007039, 61001074, 61127016), the Science and Technology Commission of Shanghai Municipality (STCSM) Project (10DJ1400402, 12XD1406400). We also acknowledge IME Singapore for device fabrication.

REFERENCES

1. F. Ferdous, H. Miao, D. E. Leaird, K. Srinivasan, J. Wang, L. Chen, L. T. Varghese, and A. M. Weiner, "Spectral line-by-line pulse shaping of on-chip microresonator frequency combs," Nat. Photon. **5**, 770-776 (2011).
2. D. T. Tan, P. C. Sun, and Y. Fainman, "Monolithic nonlinear pulse compressor on a silicon chip," Nat. Commun. **1**, 116 (2010).
3. M. Li, D. Janner, J. Yao, and V. Pruneri, "Arbitrary-order all-fiber temporal differentiator based on a fiber Bragg grating: design and experimental demonstration," Opt. Express **17**, 19798-19807 (2009).
4. M. Li, H.-S. Jeong, J. Azaña, and T.-J. Ahn, "25-terahertz-bandwidth all-optical temporal differentiator," Opt. Express **20**, 28273-28280 (2012).
5. M. Li and J. Yao, "Experimental demonstration of a wideband photonic temporal Hilbert transformer based on a single fiber Bragg grating," IEEE Photon. Technol. Lett. **22**, 1559-1561 (2010).
6. F. Liu, T. Wang, L. Qiang, T. Ye, Z. Zhang, M. Qiu, and Y. Su, "Compact optical temporal differentiator based on silicon microring resonator," Opt. Express **16**, 15880-15886 (2008).

7. J. Dong, A. Zheng, D. Gao, S. Liao, L. Lei, D. Huang, and X. Zhang, "High-order photonic differentiator employing on-chip cascaded microring resonators," Opt. Lett. **38**, 628-630 (2013).
8. L. Zhou, H. Chen, and A. W. Poon, "On-chip NRZ-to-PRZ format conversion using narrow-band silicon microring resonator-based notch filters," J. Lightwave Technol. **26**, 1950-1955 (2008).
9. M. Ferrera, Y. Park, L. Razzari, B. E. Little, S. T. Chu, R. Morandotti, D. J. Moss, and J. Azaña, "All-optical 1st and 2nd order integration on a chip," Opt. Express **19**, 23153-23161 (2011).
10. L. Zhou, T. Ye, and J. Chen, "Coherenet interference induced transparency in self-coupled optical waveguide-based resonators," Opt. Lett. **36**, 13-15 (2011).
11. X. Sun, L. Zhou, J. Xie, Z. Zou, L. Lu, H. Zhu, X. Li, and J. Chen, "Investigation of Coupling Tuning in Self-Coupled Optical Waveguide (SCOW) Resonators," IEEE Photon. Technol. Lett. **25**, 936-939 (2013).
12. Z. Zou, L. Zhou, X. Sun, J. Xie, H. Zhu, L. Lu, X. Li, and J. Chen, "Tunable two-stage self-coupled optical waveguide resonators," Opt. Lett. **38**, 1215-1217 (2013).
13. X. Sun, L. Zhou, X. Li, Z. Hong, J. Xie, H. Zhu, Z. Zou, L. Lu, and J. Chen, "Experimental demonstration of self-coupled optical waveguide (SCOW)-based resonators," in *17th OptoElectronics and Communications Conference (OECC 2012),* (Busan, Korea, 2012).
14. L. Zhou, J. Xie, L. Lu, Z. Zou, X. Sun, and J. Chen, "Coupled-resonator-induced-transparency in cascaded self-coupled optical waveguide (SCOW) resonators," in *the Asia Communications and Photonics Conference (ACP 2012)* (Guangzhou, 2012).
15. J. H. Lee, P. C. Teh, P. Petropoulos, M. Ibsen, and D. J. Richardson, "All-optical modulation and demultiplexing systems with significant timing jitter tolerance through incorporation of pulse-shaping fiber Bragg gratings," IEEE Photon. Technol. Lett. **14**, 203-205 (2002).
16. F. Parmigiani, P. Petropoulos, M. Ibsen, and D. J. Richardson, "All-optical pulse reshaping and retiming systems incorporating pulse shaping fiber Bragg grating," J. Lightwave Technol. **24**, 357-364 (2006).
17. R. SlavÝk, Y. Park, M. Kulishov, and R. Morandotti, "Ultrafast all-optical differentiators," Opt. Express **14**, 10699-10707 (2006).
18. M. Stratmann, T. Pagel, and F. Mitschke, "Experimental observation of temporal soliton molecules," Phys. Rev. Lett. **95**, 143902 (2005).
19. Z. Zhang, M. Dainese, L. Wosinski, and M. Qiu, "Resonance-splitting and enhanced notch depth in SOI ring resonators with mutual mode coupling," Opt. Express **16**, 4621-4630 (2008).
20. D. D. Smith, H. Chang, and K. A. Fuller, "Whispering-gallery mode splitting in coupled microresonators," J. Opt. Soc. Am. B **20**, 1967-1974 (2003).